Published in "Physical Review Letters 97: 103901, 2006"
which should be cited to refer to this work.

Photocount Statistics in Mesoscopic Optics

S. Balog, P. Zakharov, and F. Scheffold*
Department of Physics, University of Fribourg, 1700 Fribourg, Switzerland

S. E. Skipetrov†
Laboratoire de Physique et Modélisation des Milieux Condensés/CNRS, Maison des Magistères, Université Joseph Fourier, 38042 Grenoble, France

We report the first observation of the impact of mesoscopic fluctuations on the photocount statistics of coherent light scattered in a random medium. A Poisson photocount distribution of the incident light widens and gains additional asymmetry upon transmission through a suspension of small dielectric spheres. The effect is only appreciable when the average number $\bar{n}$ of photocounts becomes comparable or larger than the effective dimensionless conductance g of the sample.

Since Anderson's discovery that the propagation of a quantum particle can be blocked by disorder [1] and the subsequent realization that this "Anderson localization" can also take place for electromagnetic waves (photons) [2], the quest for observing it has become a very active field of research [3–14]. Although the observation of microwave localization in quasi-one-dimensional disordered samples [3] now seems to be accepted by the scientific community, the localization of visible light in strongly scattering, three-dimensional (3D) semiconductor powders [4] has been questioned [5]. For both light and microwaves, an efficient way of revealing localization effects is to study fluctuations and correlations (upon varying frequency for static scatterers [6–8] or time for mobile scatterers [8,9]) of the transmission coefficient T of the random sample, or even the full probability distribution of T [3,10–12].

Statistics of T, as well as many other mesoscopic optical phenomena (coherent backscattering and weak localization [13], long-range spatial intensity correlations [6], universal conductance fluctuations [14], etc.) have been understood and discussed in the framework of classical physics, without appealing to quantum mechanics. The impact of quantum-mechanical effects on the coherent backscattering of light has been demonstrated in beautiful experiments on light scattering in cold atomic clouds [15]. The quantum nature of *scatterers* (atoms) had to be taken into account to understand the low value of the coherent backscattering enhancement factor. Experimental studies revealing the quantum nature of *light* in multiple scattering have been reported only very recently [16], despite a considerable theoretical interest in this subject [17]. In particular, Kindermann *et al.* have predicted that disorder can substantially alter photon statistics of degenerate *incoherent* radiation. In the present Letter we report the first experimental observation of the impact of one of the precursors of Anderson localization—mesoscopic, long-range correlations—on the photon statistics of degenerate *coherent* light emitted by a conventional continuous laser. We interpret our results in the framework of the semiclassical theory of photoelectric detection [18], which appears to be sufficient under conditions of experiments reported here.

As first noted by Einstein 100 years ago [19], the quantum nature of light can be directly probed by the photoelectric effect. As the energy of the electromagnetic wave is quantized in portions $\hbar\omega$ (with $\hbar$ the Planck constant and ω the frequency of light), only an integer number n of such quanta (photons) can be absorbed by a photoelectric effect-based detector during a given time interval τ. Today's electronic equipment allows us to measure n in a wide dynamic range and to determine the probability distribution of photocounts $P(n, \bar{n})$, where $\bar{n}$ is the average number of photocounts in the interval $\tau = \bar{n}/f$ and f is the average photocount rate (number of counts per unit time). $P(n, \bar{n})$ carries fundamental information about interaction of light with the medium. In a "random laser", for example, $P(n, \bar{n})$ can be used to characterize different regimes of lasing [20]. In a different domain of physics—mesoscopic electronics—the "full counting statistics" of electrons in disordered conductors is also under active study [21].

In our experiment we measure the distribution of photocounts of laser light transmitted through an optically dense slab (see Fig. 1). The sample cell (thickness $L \approx 0.5$ mm) is filled with a charge stabilized aqueous colloidal dispersion of a commercial titanium dioxide powder (Warner Jenkinson Europe Ltd.), particle diameter $\approx$200–300 nm, at an initial density of $18 \pm 1\%$ per volume. To further increase the density we let the sealed suspension settle under gravity. Because of the electrostatic repulsion between the particles, the sedimentation is asymptotically slowed down and an equilibrium layer of $\sim$0.2–0.25 mm thickness (volume fraction ca. 35%–40%) is formed after about 10 hours. From diffusing-wave spectroscopy measurements we have checked that the particles in this layer remain mobile and undergo Brownian motion. Following the approach described in Ref. [9] we estimate the trans-

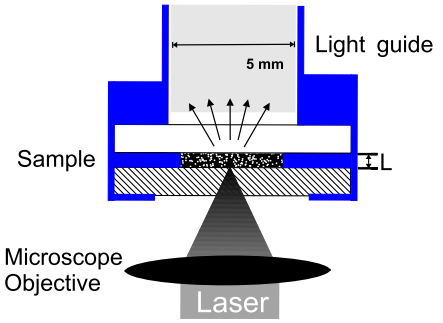

FIG. 1 (color online). Experimental setup: The incident laser beam is focused on the vertically oriented sample holder. The glass window directed towards the laser is highly absorbing while the opposite window is transparent. The windows hold a sealed liquid layer (thickness L) of colloidal titanium dioxide suspended in water. Light transmitted through the sample is collected by a light guide and recorded by a single photon detector (not shown).

port mean free path at this density to $l^* = 0.7 \pm 0.1\ \mu$m. Our sample is therefore deep in the multiple scattering regime: a typical transmitted photon experiences $(L/l^*)^2 \sim 10^5$ elastic scattering events, whereas the coherent incident beam is destroyed after a distance $l^* \ll L$ and hence does not contribute to the measured signal. The glass window directed towards the laser is highly absorbing (transmission coefficient $\simeq 0.001$) in order to suppress multiple reflections [9] while the opposite one is transparent. A frequency doubled Nd:YV04 laser ("Verdi" from Coherent) operating at the wavelength $\lambda = 532$ nm illuminates the sample through a microscope objective that focuses the laser beam to a small spot (spot size $w \gtrsim 3\ \mu$m) on the sample surface. The light transmitted through the cell is collected by a light guide (core diameter 5 mm), recorded by a single photon detector with short dead time, and processed by a digital photon counter (correlator.com, New Jersey, USA). The high temporal resolution (12.5 ns) of the latter assures that no more than one photon is arriving every time step for a typical photon count rate f of 9 MHz. In a typical experiment the photon trace is recorded over 1 h. From the recorded data we compute the probability distribution $P(n, \bar{n})$ and the time averaged correlation function of total transmission $C_2(t) = \langle T(0)T(t)\rangle/\bar{T}^2 - 1$ following standard procedures [22]. To suppress contributions from slow drifts the data is analyzed in 30 s intervals and subsequently averaged. Some representative results for different beam spot sizes are shown in Figs. 2 and 3.

Because the detection process is of probabilistic nature, the detection of a photon is a random event and $P(n, \bar{n})$ is expected to be the Poisson probability distribution [18]. However, as follows from Fig. 2, this is only true when the incident laser beam is sufficiently wide. For a focused beam we observe that the distribution widens and becomes more asymmetric than one would expect for the Poisson distribution. This indicates that additional fluctuations ex-

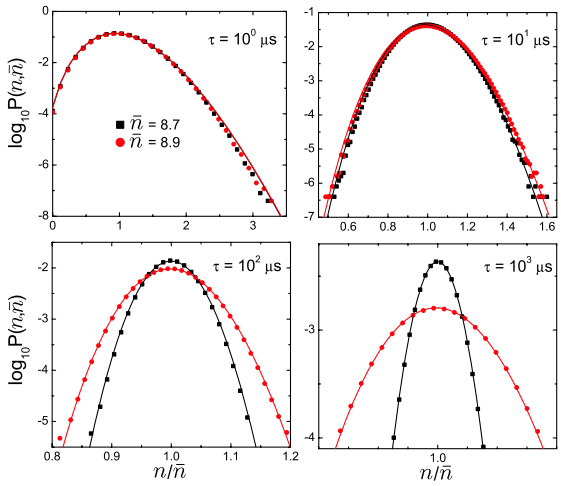

FIG. 2 (color online). Probability distributions of photon counts for an expanded incident beam (black squares) and a focused beam (beam waist $w = 3.4\ \mu$m, red circles) for four different sampling times τ. The former distribution follows the Poisson law (black line), while the latter one is well described by the Fourier transform of our Eq. (3) (red line). Small deviations for the shortest τ can be explained by the finite detector dead time [26]. The number of data points for the two longest τ has been reduced to improve readability.

ist in the latter case. These additional fluctuations are due to the random motion of scatterers. Since we collect all the transmitted intensity (total transmission measurements), and since the surface of our sample is much larger than the typical size $\sim\lambda$ of speckle spots, one could naively expect spatial speckle to average out, as it is indeed the case for large w. However, if w is small and the scattering is sufficiently strong, coherent interferences of scattered light give rise to weak but long-range correlation of distant speckle spots, which acquire a synchronous component in

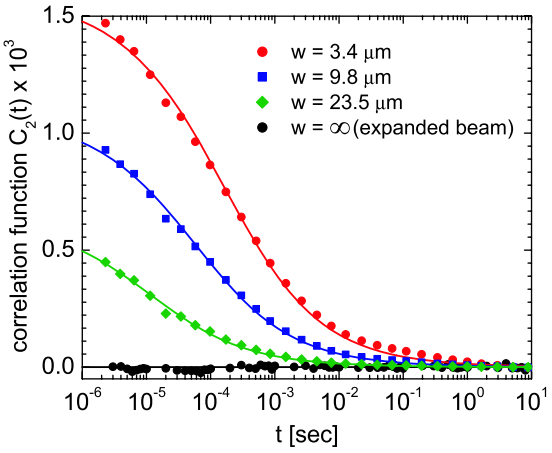

FIG. 3 (color online). Correlation function of total transmission T for different beam spot sizes w (distance between $1/e$ intensity values of a focused Gaussian beam). Lines are fits to the data.

their fluctuations. This results in enhanced fluctuations of the total transmitted signal [7,9,10].

The enhanced fluctuations of the total transmission T can be studied assuming that light is a classical wave described by Maxwell equations [10,23]. As long as localization effects are weak, the statistical distribution $P_T(T)$ of T appears to be very close to Gaussian (because the many speckle spots contributing to T are only weakly correlated and the central limit theorem applies), but with enhanced second and nonzero third central moments $M_T^{(2)}$ and $M_T^{(3)}$, where $M_T^{(k)} = \langle (T-\bar{T})^k \rangle / \bar{T}^k$. Therefore, the characteristic function of T can be approximated by

$$\chi_T(q) = \exp\left(i\bar{T}q - \frac{1}{2}\bar{T}^2 M_T^{(2)} q^2 - \frac{i}{6}\bar{T}^3 M_T^{(3)} q^3 \right). \quad (1)$$

When the measurement of T is not instantaneous but involves time integration, the second moment is given by [18]

$$M_T^{(2)} = \frac{2}{\tau}\int_0^\tau \left(1 - \frac{t}{\tau}\right) C_2(t)\,dt. \quad (2)$$

The third moment $M_T^{(3)}$ of the distribution of T can be shown to be proportional to the square of the second one: $M_T^{(3)} = \alpha M_T^{(2)2}$, where the proportionality constant $\alpha = 16/5$ for a wide ($w \gg L$) Gaussian beam [23]. The limit $w \geq L$ has also been studied both in frequency- [7] and time-domain [9] correlation experiments. In our experiments, on the contrary, the beam width w is much smaller than the thickness L of the sample (typically, $w/L \sim 10^{-2}$). In this situation, by performing calculations similar to that of Ref. [7] we find $C_2(t) = (2/3g)\exp(3t/4t_0) \times [1 - \Phi(\sqrt{3t/4t_0})]$, where Φ is the error function [24]. Leaving the discussion of the microscopic expressions for g and t_0 for a future publication, we just note here that g scales with the beam spot size w and hence the magnitude of the total transmission fluctuations ($\sim 1/g$) can be varied by adjusting w, similarly to the wide-beam situation [7,9]. By analogy with the case of the disordered waveguide [3,11,12], we will further term g the "effective" dimensionless conductance. The above expression for $C_2(t)$ with $g \sim 10^3$ and $t_0 \sim 10^{-5}$–10^{-4} s provides a good fit to our measurements (see Fig. 3).

According to the famous Mandel's formula [18], the statistical distribution of photocounts $P(n,\bar{n})$ can be obtained by averaging the Poisson distribution $P_{\text{Poisson}}(n, \bar{n} = \eta T)$ over the distribution $P_T(T)$ of the total transmission T, with η the quantum efficiency of the photodetector. The Fourier transform of the Mandel's formula with respect to n yields a relation between the characteristic functions $\chi_n(q)$ and $\chi_T(q)$:

$$\chi_n(q) = \chi_T[i\bar{n}(1 - e^{iq})/\bar{T}]$$
$$\simeq \exp\left(i\bar{n}q - \frac{1}{2}\bar{n}^2 M_n^{(2)} q^2 - \frac{i}{6}\bar{n}^3 M_n^{(3)} q^3 \right), \quad (3)$$

where the second line is obtained by expanding the first one in power series in q, which is justified for large $\bar{n}$. The second and the third central moments of n in Eq. (3) are

$$M_n^{(2)} = \frac{1}{\bar{n}} + M_T^{(2)}, \quad (4)$$

$$M_n^{(3)} = \frac{1}{\bar{n}^2} + M_T^{(3)} + 3\frac{M_T^{(2)}}{\bar{n}}. \quad (5)$$

The Fano factor is $F = (\langle n^2 \rangle - \bar{n}^2)/\bar{n} = 1 + \bar{n} M_T^{(2)} > 1$, which indicates photon bunching. The photocount distribution $P(n,\bar{n})$ obtained by the Fourier transform of Eq. (3) describes our measurements very well (see Fig. 2) when we use the fits to the correlation function $C_2(t)$ obtained independently (Fig. 3) to determine $M_T^{(2)}$ and $M_T^{(3)}$. Note that there is no trivial relation between our $P(n,\bar{n})$ and $P_T(T)$ studied previously for light [10] and microwaves [11] in transmission through *static* disordered samples. In our experiments the microscopic configuration of scatterers changes *during* the time τ that it takes to accumulate n photons, whereas T is the value of the transmission coefficient corresponding to a given (fixed) configuration of scatterers, and $P_T(T)$ of Refs. [10,11] does not contain any information about the decorrelation of T with time.

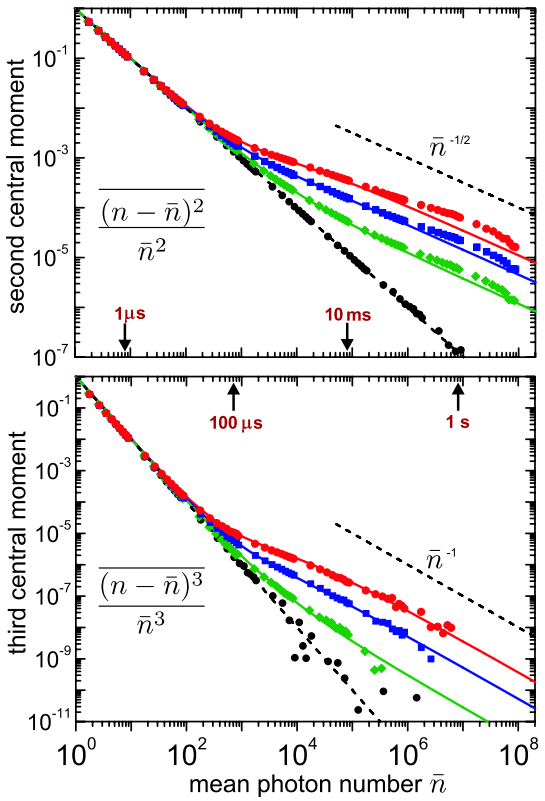

FIG. 4 (color online). Second and third central moments of the photocount distribution $P(n,\bar{n})$ for the same beam spot sizes as in Fig. 3. Lines are theoretical results (4) and (5). The third moment plot is a fit to the data with $\alpha = 3.02$, 2.59, and 2.00 (for curves from top to bottom).

The first terms on the right-hand sides of Eqs. (4) and (5) correspond to the results expected for Poisson distribution of photocounts. As we show in Fig. 4, these results are recovered for small $\bar{n} \ll g$, when the photocount distribution is dominated by the shot noise due to the discreteness of n and is not sensitive to the randomness of the scattering medium. Deviations from the Poisson-like behavior start to become important when $\bar{n}$ becomes comparable to the effective dimensionless conductance g. The long-range character of the correlation function $C_2(t) \sim 1/\sqrt{t}$ is responsible for new scaling laws $M_n^{(2)} \sim 1/\sqrt{\bar{n}}$ and $M_n^{(3)} \sim 1/\bar{n}$ in the limit of large $\bar{n}$. This behavior is well confirmed by our measurements: as can be seen in Fig. 4, the data points indeed follow the $1/\sqrt{\bar{n}}$ and $1/\bar{n}$ asymptotes shown by dashed lines [25]. Mesoscopic fluctuations of the total transmission T due to the random motion of scatterers in the disordered sample become dominant in this regime, whereas the shot noise is negligible. We see therefore that the transition between small- and large-$\bar{n}$ regimes in $P(n, \bar{n})$ is governed by localization effects, the strength of the latter being measured by the dimensionless conductance g.

In conclusion, mesoscopic fluctuations of coherent light transmission through a random medium produce measurable deviations of photocount distribution $P(n, \bar{n})$ from Poisson law, provided that the average number of photocounts $\bar{n}$ is comparable or larger than the effective dimensionless conductance g of the random sample. An interesting continuation of this work would be to analyze $P(n, \bar{n})$ for incident light in chaotic or in *nonclassical* (Fock, squeezed, etc.) states. Our preliminary calculations show that for the incident light in the single mode one-photon Fock state $M_n^{(2)} = 1/\bar{n} - 1$, i.e., the photon number fluctuations are suppressed below the $1/\bar{n}$ shot-noise limit and are independent of the fluctuations of T. On the other hand, for a single mode chaotic incident beam $M_n^{(2)} = 1/\bar{n} + 1 + 2M_T^{(2)}$, provided that the coherence time of the beam exceeds the sampling time τ.

This work was financially supported by the Swiss National Science Foundation (Project No. 200021-101620). S. E. S. acknowledges financial support of INTAS at the early stages of this work.

*Electronic address: Frank.Scheffold@unifr.ch
†Electronic address: Sergey.Skipetrov@grenoble.cnrs.fr

[1] P. W. Anderson, Phys. Rev. **109**, 1492 (1958).
[2] S. John, Phys. Rev. Lett. **53**, 2169 (1984); P. W. Anderson, Philos. Mag. B **52**, 505 (1985); S. John, Phys. Today **44**, No. 5, 32 (1991).
[3] A. A. Chabanov, M. Stoytchev, and A. Z. Genack, Nature (London) **404**, 850 (2000); A. A. Chabanov and A. Z. Genack, Phys. Rev. Lett. **87**, 153901 (2001).
[4] D. S. Wiersma *et al.*, Nature (London) **390**, 671 (1997).
[5] Comment on Ref. [4]: F. Scheffold *et al.*, Nature (London) **398**, 206 (1999); Reply to Comment: D. S. Wiersma *et al.*, *ibid.* **398**, 207 (1999).
[6] A. Z. Genack, N. Garcia, and W. Polkosnik, Phys. Rev. Lett. **65**, 2129 (1990).
[7] M. P. Van Albada, J. F. de Boer, and A. Lagendijk, Phys. Rev. Lett. **64**, 2787 (1990); J. F. de Boer, M. P. van Albada, and A. Lagendijk, Phys. Rev. B **45**, 658 (1992).
[8] E. Akkermans and G. Montambaux, *Physique Mésoscopique des électrons et des Photons* (EDP Sciences/ CNRS Editions, Paris, 2004).
[9] F. Scheffold *et al.*, Phys. Rev. B **56**, 10 942 (1997).
[10] J. F. de Boer *et al.*, Phys. Rev. Lett. **73**, 2567 (1994).
[11] M. Stoytchev and A. Z. Genack, Phys. Rev. Lett. **79**, 309 (1997); Opt. Lett. **24**, 262 (1999).
[12] A. Z. Genack and A. A. Chabanov, J. Phys. A **38**, 10 465 (2005).
[13] M. P. van Albada and A. Lagendijk, Phys. Rev. Lett. **55**, 2692 (1985); P.-E. Wolf and G. Maret, *ibid.* **55**, 2696 (1985); E. Akkermans, P. E. Wolf, and R. Maynard, *ibid.* **56**, 1471 (1986).
[14] F. Scheffold and G. Maret, Phys. Rev. Lett. **81**, 5800 (1998).
[15] G. Labeyrie *et al.*, Phys. Rev. Lett. **83**, 5266 (1999); T. Jonckheere *et al.*, *ibid.* **85**, 4269 (2000).
[16] P. Lodahl and A. Lagendijk, Phys. Rev. Lett. **94**, 153905 (2005).
[17] M. Patra and C. W. J. Beenakker, Phys. Rev. A **60**, 4059 (1999); **61**, 063805 (2000); C. W. J. Beenakker, M. Patra, and P. W. Brouwer, *ibid.* **61**, 051801 (2000); M. Kindermann, Yu. V. Nazarov, and C. W. J. Beenakker, Phys. Rev. Lett. **88**, 063601 (2002); P. Lodahl, A. P. Mosk, and A. Lagendijk, *ibid.* **95**, 173901 (2005).
[18] L. Mandel and E. Wolf, *Optical Coherence and Quantum Optics* (Cambridge University Press, Cambridge, England, 1995).
[19] A. Einstein, Ann. Phys. (Berlin) **17**, 132 (1905).
[20] H. Cao *et al.*, Phys. Rev. Lett. **86**, 4524 (2001); M. Patra, Phys. Rev. A **65**, 043809 (2002); L. Florescu and S. John, Phys. Rev. Lett. **93**, 013602 (2004).
[21] C. W. J. Beenakker and M. Büttiker, Phys. Rev. B **46**, R1889 (1992); L. S. Levitov, H. Lee, and G. B. Lesovik, J. Math. Phys. (N.Y.) **37**, 4845 (1996); D. A. Bagrets, Phys. Rev. Lett. **93**, 236803 (2004).
[22] K. Schätzel, Quantum Opt. **2**, 287 (1990).
[23] M. C. W. van Rossum, J. F. de Boer, and Th. M. Nieuwenhuizen, Phys. Rev. E **52**, 2053 (1995); M. C. W. van Rossum and Th. M. Nieuwenhuizen, Rev. Mod. Phys. **71**, 313 (1999).
[24] The frequency and time correlation functions $C_2(\Delta\omega)$ and $C_2(t)$ can be calculated in very similar ways, but the final result for $C_2(t)$ cannot be trivially deduced from $C_2(\Delta\omega)$ [8].
[25] We attribute the slight curvature of experimental curves in Fig. 4 to slow fluctuations and drifts of the laser intensity on a time scale of the order of minutes. Though already extremely small in our experiments, these effects cannot be completely suppressed.
[26] F. A. Johnson *et al.*, Phys. Rev. Lett. **16**, 589 (1966).